Journal of Electroceramics 1:2, 155–164, 1997

Ceria-Zirconia Composite Electrolyte for Solid Oxide Fuel Cells

TERUHISA HORITA, NATSUKO SAKAI, HARUMI YOKOKAWA, MASAYUKI DOKIYA, TATSUYA KAWADA[1], JAN VAN HERLE[2], & KAZUTAKA SASAKI[3]

National Institute of materials and Chemical Research 1-1 Higashi, Tsukuba, 305 Japan, (1) Tohoku University, (2) École Polytechnique Fédérale De Lausanne, (3) Imperial College of Science, Technology and Medicine

Submitted July 23, 1996; Revised March 19, 1997; Accepted April 3, 1997

Abstract. Ceria-zirconia-ceria sandwich structured composite film electrolytes were designed in order to offer high ionic and low electronic conductivity electrolyte films. Calculation of oxygen potential profile in the composite film electrolyte indicates that a very thin zirconia film kills the electronic current of ceria without affecting the ionic conductivity. The composite films were successfully prepared by a co-fire process. The main problem was the fact that the ceria and zirconia green films had different shrinkage behaviors. Successful co-firing was achieved by controlling the temperature program and amount of binder. De-lamination between yttria stabilized zirconia(YSZ) and gadolinia doped ceria(GDC) layers was overcome by the formation of a solid solution phase at the interface of the two films. The resultant composite films, however, showed poor electrical conductivity compared with theoretical values. The formation of a solid solution phase can have a negative effect on composite electrolytes. Also, the composite film is unsatisfactory in terms of mechanical strength. This could be due to the lattice expansion in reducing atmospheres, thermal expansion coefficient mismatch, or the intrinsic weakness of the ceria texture.

Keywords: solid oxide fuel cells, ceria-zirconia electrolyte, co-fire, mixed conduction, solid solution

1. Introduction

Solid oxide fuel cells (SOFCs) usually operate at around 1123–1323 K. A recent research target is to reduce this high operational temperature to 773–873 K or 973–1073 K. A decrease to 773–873 K is favorable for applications in electric vehicles using methanol fuel [1]. A decrease to 973–1073 K is a more practical target than the former case, allowing the use of alloys as separator materials in order to reduce cost, to make fast heat removal possible, to increase mechanical strength, etc. The present study relates to the latter case. For these purposes, we need an alternative electrolyte which has higher ionic conductivity than yttria stabilized zirconia (YSZ) and more active electrodes than those used for YSZ electrolytes. Rare earth oxide doped ceria (RDC, R is usually Y_2O_3, Gd_2O_3, and Sm_2O_3) is considered to be a candidate electrolyte due to its superior ionic conductivity.

RDC is considered to be preferable as an electrolyte not only because of its high ionic conductivity but also due to the following properties.

1. RDC has higher thermal expansion coefficient (TEC $\sim 12 \times 10^{-6}$ m/mK) than YSZ (TEC $\sim 10 \times 10^{-6}$ m/mK), which is more compatible when used with Fe-Cr alloys (TEC $> 12 \times 10^{-6}$ m/mK).
2. RDC will show higher electrode compatibility than YSZ. When RDC is used as an electrolyte, $La(Fe,Co)O_3$, which is more active than $LaMnO_3$, can be used as a cathode material and Ni-YSZ cermet anodes are also expected to show higher performance on RDC than on YSZ electrolyte [2,3].

However, it is well known that, RDC has high electronic conductivity which leads to lower open circuit voltage (OCV) and to higher electrochemical oxygen permeation than in case of YSZ [4]. Therefore a coating of YSZ at the reducing side prepared by a ''dry process'', RF ion plating [2], or sputtering [5], etc., has been considered to prevent the oxygen

permeation. In order to offer cheaper YSZ coating process, ''wet process'' is preferable in the practical application. Fabrication of a two layer YSZ-RDC composite film was very difficult in the wet-process, because of the difference of the thermal expansion and shrinkage behavior mismatch. Hence, we designed a composite electrolyte which has a sandwich structure, ''RDC-YSZ-RDC'', as shown in Fig. 1. Such a sandwich structure has the following advantages:

1. A thin YSZ film will block the electronic current.
2. If the YSZ film is thin enough, its higher ionic resistance will be negligible compared with the RDC electrolyte.
3. The surface of RDC electrolytes will offer higher electrode activity for both anode and cathode.
4. If the YSZ film is sufficiently thin, its TEC will accommodate that of the RDC electrolyte.
5. A symmetrical sandwich structure is easier to fabricate, cutting down cost for the co-fire process.

The purpose of the present study is to examine the feasibility of ceria-zirconia-ceria three layer composite electrolytes and to fabricate this sandwich structured electrolyte by wet co-firing process.

2. Feasibility of Ceria-Zirconia-Ceria Composite Electrolyte

2.1. Theoretical Calculation Procedure

Let us assume a sandwich structured composite film of RDC and YSZ as shown in Fig. 1. The analysis of the oxygen chemical potential profile in the composite film is indispensable to estimate the electrochemical properties (open circuit voltage (OCV) and current–voltage characteristics) and lattice expansion of RDC in reducing atmosphere. Choudhury and Patterson [6] analyzed the oxygen chemical potential profile of mixed conductors and proposed the introduction of a parameter r as,

$$r = \frac{J(\mathrm{O}^{2-})}{J(e)} \tag{1}$$

where $J(\mathrm{O}^{2-})$ is the oxide ion flux through the electrolyte, $J(\mathrm{e})$ is the electron flux through the electrolyte. Here, $r = -1$ at open circuit and $|r| > 1$ at SOFC operation condition.

Calculation for mono-layer electrolyte. Basic equations are presented for calculation of the oxygen potential profile inside the mono-layer electrolyte. For simplicity, the calculation is set as one dimensional direction along to x, from low to high oxygen partial pressure, as illustrated in Fig. 1. Every basic equation is written as a function of the oxygen partial pressure. The ionic current density, $J(\mathrm{O}^{2-})$ is written in the following:

$$J(\mathrm{O}^{2-}) = \frac{\sigma(\mathrm{O}^{2-})}{2F}\frac{\partial\eta(\mathrm{O}^{2-})}{\partial x} = rJ(\mathrm{e}) = \frac{RT}{4F}\frac{r\sigma(\mathrm{e})\sigma(\mathrm{O}^{2-})}{r\sigma(\mathrm{e}) - \sigma(\mathrm{O}^{2-})}\frac{\partial \ln P(\mathrm{O}_2)}{\partial x} \tag{2}$$

where $\sigma(\mathrm{O}^{2-})$ is the oxide ionic conductivity of the electrolyte, $\sigma(\mathrm{e})$ is the electronic conductivity of the electrolyte, R is the gas constant, T is cell temperature, and F is the Faraday constant. In an integrated form, oxide ionic flux can be written as:

$$J(\mathrm{O}^{2-})x = \frac{RT}{4F}\int_{p_1(\mathrm{O}_2)}^{p_2(\mathrm{O}_2)} \times \frac{r\sigma(\mathrm{e})\sigma(\mathrm{O}^{2-})}{r\sigma(\mathrm{e}) - \sigma(\mathrm{O}^{2-})} d\ln P(\mathrm{O}_2) \tag{3}$$

where, x is the distance into the electrolyte from low to high oxygen partial pressure, $P_1(\mathrm{O}_2)$ is oxygen partial pressure at lower side, and $P_2(\mathrm{O}_2)$ is oxygen partial pressure at a point a distance x from the origin. Total external current density, J_{ext} is thus expressed in the following equation:

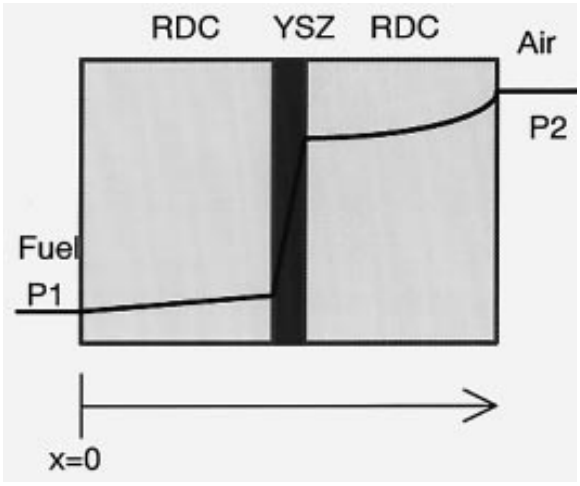

Fig. 1. Scheme of ceria-zirconia-ceria 3 layer composite. (RDC: Rare earth oxide Doped Ceria, YSZ: Yttria Stabilized Zirconia, line indicates the schematic drawing the oxygen potential profile inside the 3 layer composite electrolyte placed between fuel and air atmosphere)

$$J_{\text{ext}} = J(\text{O}^{2-}) + J(\text{e}) = \frac{(1+\text{r})\text{RT}}{4\text{FL}} \times \int_{p_1(\text{O}_2)}^{p_2(\text{O}_2)} \frac{\sigma(\text{e})\sigma(\text{O}^{2-})}{r\sigma(\text{e}) - \sigma(\text{O}^{2-})} d\ln P(\text{O}_2) \quad (4)$$

J_{ext} is the external current from the cell, L is the electrolyte thickness. This equation gives the oxygen potential profiles inside the electrolyte when changing the r value (the ratio of ionic and electronic current). On the other hand, terminal voltage is calculated from the gradient of the electrochemical potential ($\partial\eta(\text{e})/\partial x$). The gradient of the electrochemical potential of electron is written as follows;

$$\frac{\partial\eta(\text{e})}{\partial x} = \frac{RT}{4} \frac{\sigma(\text{O}^{2-})}{r\sigma(\text{e}) - \sigma(\text{O}^{2-})} \frac{\partial \ln P(\text{O}_2)}{\partial x} \quad (5)$$

The terminal voltage is obtained by integrating the electrochemical potential as a function of the oxygen partial pressure:

$$V = \frac{-RT}{4F} \int_{p_1(\text{O}_2)}^{p_2(\text{O}_2)} \frac{\sigma(\text{O}^{2-})}{r\sigma(\text{e}) - \sigma(\text{O}^{2-})} d\ln P(\text{O}_2) \quad (6)$$

Calculation for 3-layer composite electrolyte. The calculation was carried out for 1073 K, based on the following ionic and electronic conductivities of gadolinia doped ceria (GDC) and YSZ [2,7]. The ratio of the electrolyte thickness is set as t(GDC)/t(YSZ)/t(GDC)=10/1/10 in this calculation.

$\text{Ce}_{0.8}\text{Gd}_{0.2}\text{O}_{1.9}$ (GDC):

$$\sigma(\text{O}^{2-}) = 0.0520\ \text{Scm}^{-1},$$

$$\sigma(\text{e}) = 2.24 \times 10^{-7}\ \text{P}(\text{O}_2)^{-1/4}$$

$(\text{Y}_2\text{O}_3)_{0.08}(\text{ZrO}_2)_{0.92}$ (YSZ):

$$\sigma(\text{O}^{2-}) = 0.0251\ \text{Scm}^{-1},$$

$$\sigma(\text{e}) = 5.62 \times 10^{-13}\text{P}(\text{O}_2)^{-1/4} + 1.78 \times 10^{-10} P(\text{O}_2)^{1/4}$$

The calculation procedure is schematically illustrated in Fig. 2. The equation (3) gives $J(\text{O}^{2-})x$ as a function of the oxygen partial pressure. Since the oxide ion flux $J(\text{O}^{2-})$ in the 3 layer is constant under steady state conditions, $J(\text{O}^{2-})x$ value indicates the position inside the electrolyte. The integrated ranges of oxygen potentials in Eq. (3) are divided into three, whose boundaries of oxygen potentials are $p_1(\text{O}_2)$, $p'(\text{O}_2)$, $p''(\text{O}_2)$, and $p_2(\text{O}_2)$ ($p_1(\text{O}_2) < p'(\text{O}_2) < p''(\text{O}_2) < p_2(\text{O}_2)$). Each integration gives the dimension of flux times thickness, such as $J(\text{O}^{2-})x$ [Acm^{-1}]. Thus $J(\text{O}^{2-})x_{GDC(1)}$ can be calculated from $p_1(\text{O}_2)$ to higher oxygen potential boundary $p'(\text{O}_2)$, as follows.

$$J(\text{O}_2)x_{GDC(1)} = \frac{RT}{4F} \int_{p_1(\text{O}_2)}^{p'(\text{O}_2)} \frac{r\sigma(\text{e})\sigma(\text{O}^{2-})}{r\sigma(\text{e}) - \sigma(\text{O}^{2-})} d\ln P(\text{O}_2) \quad (7)$$

The integration of Eq. (3) also starts from $p_2(\text{O}_2)$ to lower oxygen potential boundary of another point, $p''(\text{O}_2)$, so as to be same value of $J(\text{O}_2)x_{GDC(1)}$, as follows:

$$J(\text{O}_2)x_{GDC(2)} = \frac{RT}{4F} \int_{p_2(\text{O}_2)}^{p''(\text{O}_2)} \frac{r\sigma(\text{e})\sigma(\text{O}^{2-})}{r\sigma(\text{e}) - \sigma(\text{O}^{2-})} d\ln P(\text{O}_2) \quad (8)$$

Between $p'(\text{O}_2)$ and $p''(\text{O}_2)$, the integration of YSZ-part is performed with the same integration Eq. (3):

$$J(\text{O}_2)x_{YSZ} = \frac{RT}{4F} \int_{p'(\text{O}_2)}^{p''(\text{O}_2)} \frac{r\sigma(\text{e})\sigma(\text{O}^{2-})}{r\sigma(\text{e}) - \sigma(\text{O}^{2-})} d\ln P(\text{O}_2) \quad (9)$$

According to the boundary condition, $J(\text{O}^{2-})x_{GDC(2)}$ must be same value of $J(\text{O}^{2-})x_{GDC(1)}$, and $J(\text{O}^{2-})x_{GDC(1)}$ should be 10 times higher than $J(\text{O}^{2-})x_{YSZ}$. The boundary oxygen potential of $p'(\text{O}_2)$ and $p''(\text{O}_2)$ are shifted from $p_1(\text{O}_2)$ and $p_2(\text{O}_2)$ slightly, and compare the each $J(\text{O}^{2-})x$ value. This procedure is repeated until each value meets the boundary condition.

2.2. Results

Figure 3 shows the oxygen potential profiles within the GDC-YSZ-GDC laminate sandwich structure with a thickness ratio of t(GDC)/t(YSZ)/t(GDC)=10/1/10 under open circuit and current flow conditions. The oxygen potential profiles were plotted as a function of normalized thickness, because the calculated $J(\text{O}^{2-})x$ value indicates the position inside the electrolyte under constant $J(\text{O}^{2-})$. At open circuit (line (1) in Fig. 3) and/or at practical current densities (lines (2) and (3) in Fig. 3), the oxygen potential profile is relatively flat in the GDC region on the reducing side, followed by a large increase in gradient in the YSZ region. This

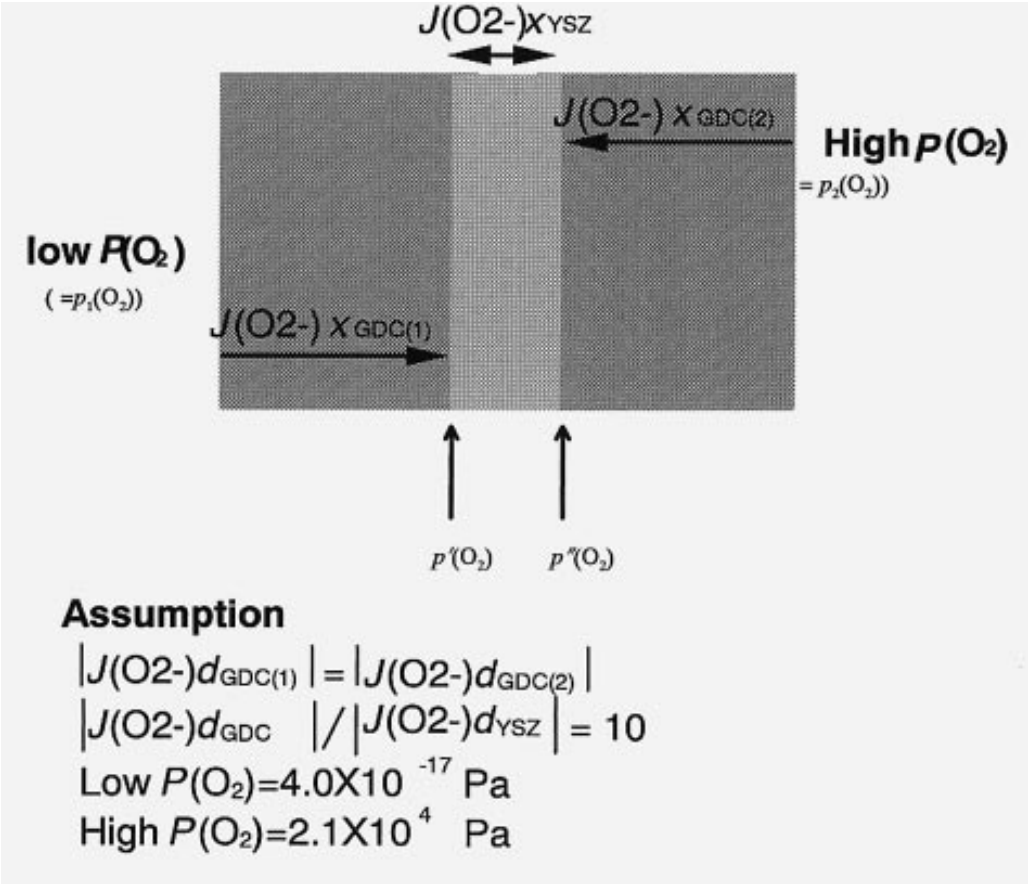

Fig. 2. Schematic illustration of the calculation procedure for oxygen potential profile inside the ceria-YSZ-ceria three composite electrolyte.

oxygen potential profile at practical J_{ext} suggests that YSZ will effectively block electronic current without reducing the OCV (line (a), Fig. 4). When the YSZ film is very thin, its ionic resistance will be negligibly small. Thus, the ionic conductivity of the composite electrolyte films will be dominated by RDC electrolytes, whilst the electronic conductivity is determined by YSZ. Figure 4 simulates a cell performance of composite GDC-YSZ-GDC and GDC film electrolyte: This simulation only includes the ohmic resistance of the electrolyte and neglects the polarization at electrodes, because the overvoltage of the electrode is sometimes influenced by many factors, such as electrode kinetics. Since the electrode performance on the GDC electrolyte can be expected to be better than on the YSZ electrolyte [2], this result suggests better cell performance of GDC-YSZ-GDC composite electrolyte than GDC or YSZ mono-layer electrolytes.

3. Fabrication of Co-Fired multi-layer Composite Electrolyte

3.1. Experimental

Powders. Commercially available GDC (Anan Kasei Co. Ltd., JAPAN) was calcined (1073–1273 K, 1 h) and ball milled (polyethylene container with YSZ ball, milling over 48 h). Some YSZ powders, such as Tosoh-3Y, -8Y and Zircar-4Y, were tested, but they did not give good shrinkage matching. Among them, Zircar-4Y showed similar shrinkage behavior to GDC, and it was used in the co-fire process (see Fig. 5).

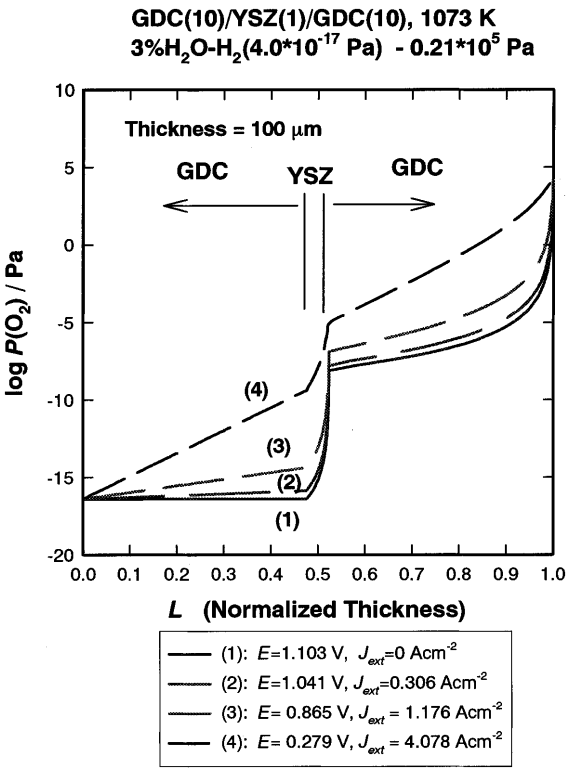

Fig. 3. Calculated oxygen potneitla profiles inside the GDC/YSZ/GDC 3 layer composite electrolyte under open circuit and current flow condition. (a) 1073 K, total thickness = 100 μm, (1) open circukt, (2) Terminal Voltage $E = 1.041$ V and Current density $J_{ext} = 0.306\,Acm^{-2}$, (3) $E = 0.865$ V, $J_{ext} = 1.176\,A\,cm^{-2}$, (4) $E = 0.280$ V, $J_{ext} = 4.08\,Acm^{-2}$).

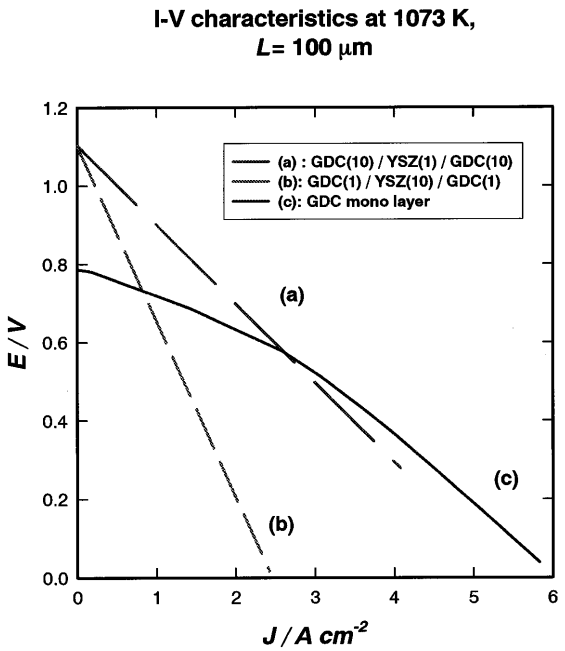

Fig. 4. Expected I–V curves of cells (total electrolyte thickness is 100 μm). (a): GDC (10)/YSZ(1)/GDC (10), (b): GDC(1)/YSZ(10)/GDC(1), (c): GDC mono layer. Number in the blacket indicates the ratio of the thickness of each layer.

Doctor blade. Slurries of GDC and YSZ were prepared by ball milling (polyethylene container with YSZ ball) the following mixtures: Ceramic powders (100 g), binder (poly-vinyl-butyral, 10 g), plasticizer (di-n-butyl phthalate, 10 cm^3), fish oil (2 cm^3), triton X (Polyethylene Glycol Mono-*p*-isooctylphenyl Ether (2 cm^3), and solvent (isopropanol 50 cm^3, toluene 25 cm^3). For YSZ, the amount of binder was 3 times greater than GDC in order to increase the adheriveness to obtain a thin film, and for shrinkage matching during sintering. After controlling the viscosity of the slurries, the doctor blade process was used with blade slits of 500 μm for GDC and 300 μm for YSZ. Multi-layer green tapes were prepared by overlapping doctor blade coatings or by manually sticking GDC and YSZ green tapes into the desired sandwich structures such as GDC-YSZ-GDC.

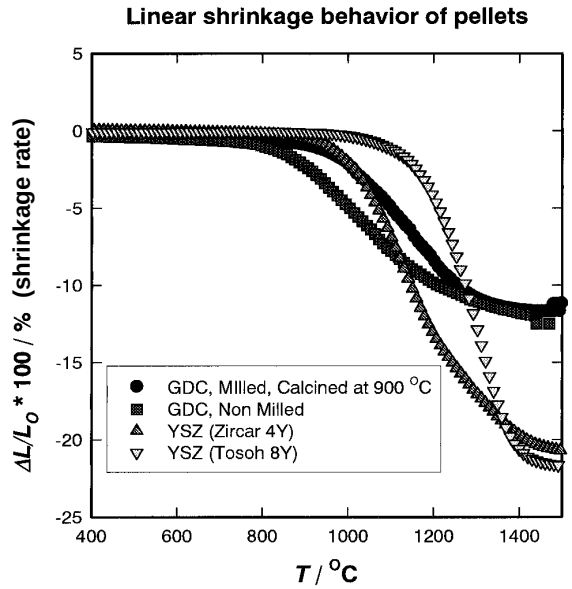

Fig. 5. Linear shrinkage behaviour of green GDC and YSZ pellet samples. [ΔL: shrinkage length of the green pellets, ●: GDC (Calcined at 1173 K and milled), ■: GDC (Non milling), ▲ YSZ (Zircar-4Y), ▽: YSZ (Tosoh, TZ-8Y)].

No differences were observed between multi-layer films prepared by the overlapping doctor blade coating and by manually sticking the green tapes.

De-waxing, calcining, and co-fire. The shrinkage behavior of powders were examined by a thermo-mechanical-analyzer (TMA320, SEIKO Instruments Co., Ltd.) using $4 \times 4 \times 2$ mm samples cut from pellets (pelletized at 0.2 MPa). The shrinkage behavior of green tapes were examined by quenching samples during calcining and/or co-fire process.

Green films were de-waxed by the temperature program as illustrated in Fig. 6(a), and then calcined by several temperature programs. The optimal sintering temperature program was found to be as shown in Fig. 6(b).

Observation of microstructure by SEM/EDX. The microstructure and the elemental distribution of the composite films was analyzed by Scanning Electron Microscopy (SEM, Hitachi, S-800) with Energy Dispersion X-ray analysis (EDX, Kevex). The cross section of the composite film was polished by a diamond paste (up to 1/4 μm grade) to produce a flat surface.

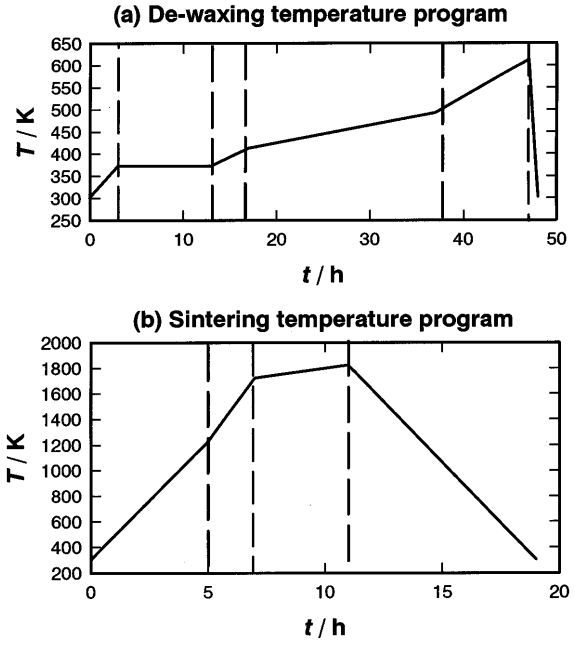

Fig. 6. Temperature program for de-waxing (a) and sintering (b) of tape cast films.

3.2. Results

Sintering behavior of powders and green tapes. Ceria is well known as an ill-sinterable material. However, it was found that by controlling the pH and concentration of the co-precipitation process it is possible to produce RDC powders which can be sintered at low temperatures (lower than 1573 K) [8,9]. It was also found that other processes, for example, a modified Pechini process or carbonate thermal decomposition process can supply powders that sinter at temperatures lower than 1673 K.

For the co-firing of two distinct ceramic layers, the shrinkage behavior of the two components must be similar. Several methods were used to match the sintering behavior of GDC and YSZ powders. It was found that slight calcining (1073–1273 K) and milling below 0.5 μm (zirconia ball in polyethylene mill for $\sim$48 h) could change the sinterability of the GDC powders. Figure 5 shows the linear shrinkage behavior of YSZ and GDC green pellets measured by TMA. Pre-calcining and milling made the sintering behavior of GDC similar to that of Zircar-4Y for starting temperatures. However, the total linear shrinkage is different between YSZ and GDC green pellets: total linear shrinkage lengths of GDC green pellets are around 12%, though that of YSZ green pellets are around 21%. The linear shrinkage difference may be influenced by the initial packing state of the green pellets before the TMA measurements. The GDC powders were so fine that the green pellets of GDC had higher density than the green pellets of YSZ. Using the GDC powders which were pre-calcined and milled, the sintering characteristics of the following green tapes were compared GDC, YSZ-4Y, and GDC-YSZ-GDC. Figure 7 shows volume change of YSZ mono-layer (triangle), GDC mono-layer (circle), and GDC-YSZ-GDC three layer (square, YSZ layer contains binder 3 times higher than the usual). The initial size of the film was usually $13 \times 13 \times$ thickness cm^3, which is set as 100% in Fig. 7. Upon de-waxing ($\sim$623 K), there was already a large difference in shrinkage between GDC and YSZ films. During sintering ($>$1223 K), YSZ started to shrink at higher temperature than GDC as shown in Fig. 7. Total volume shrinkage of these three green films are around 70–75%, which are not perfectly matching. In the present study, even by controlled precalcining and ball milling, perfectly matching shrinkage behavior was not obtained

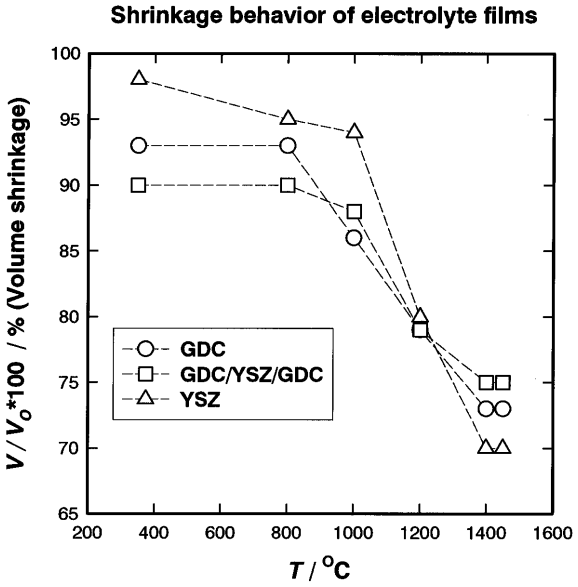

Fig. 7. Volume shrinkage behavior of each electrolyte green films. [initial volume is $13 \times 13 \times$ thickness (cm^3), $V/V_O = 100\%$, ○: GDC mono-layer green tape, □: GDC/YSZ/GDC 3 layer composite with binder rich YSZ layer (3 times more volume of binder), Δ YSZ with 3 times more volume of binder].

between YSZ and GDC films during de-waxing and sintering.

Fabrication of co-fired composite electrolytes. In the preliminary co-firing trial of GDC-YSZ-GDC composite green films, no cracks or curvatures were observed in the de-waxing step. This means that there is a fairly wide allowance in shrinkage mismatch during de-waxing. Upon co-firing, cracks appeared in the composite films. Furthermore de-lamination occurred when GDC-YSZ-GDC composite green films were fired. In some cases, no cracks appeared in the de-laminated YSZ films.

Based on the above observations, we assumed that YSZ and GDC would behave independently during co-firing, as follows: In GDC-YSZ-GDC films, the outer GDC layer films sinter first. When the outer GDC layer has densified, the inner YSZ has not yet sintered and remains porous. At this point, if the inner YSZ layer is still ''flexible'' to some extent, it would be densified between two dense GDC films, without inducing cracks. It may be said that a ''pseudo-hot-press'' condition arises. The inner YSZ film is pressed by two GDC films. Densification completes itself at 1723 K for both YSZ and GDC films. However, at this temperature the YSZ and GDC films had not joined since samples quenched at this temperature showed de-lamination.

Based on these possibilities, we introduced a binder-rich YSZ green film which contains three times more binder than the standard recipe. This produces very thin films without significantly affecting the sintering of GDC tapes, if the shrinkage of the binder rich film occurs perpendicular to the sheet. It was also conceived that the temperature program could have an improved effect on sintering behavior. We tested several temperature programs from 1223 K to 1723 K. It was found that a temperature elevation rate of 200 K/h-300 K/h is preferable, since this temperature program gave crack free de-laminated leafs of YSZ and GDC upon quenching from 1723 K. The next step was to obtain good joining between YSZ and GDC films. For this purpose, it was necessary to bring the co-fired films up to 1823 K to allow the formation of a solid solution and join the two films. For this step, a rather slow temperature elevation rate was adopted: an increase in temperature from 1723 K to 1823 K with a rate of 100 K/4 h is used (see Fig. 6).

With these techniques, we successfully made composite films by a wet co-fire process. The case shown in Fig. 8 is one example of co-fired films. Dense and thin YSZ layer was inserted between the dense and thick GDC layers. When we start with blade slit of 500 μm for GDC green film and blade slit of 300 μm for binder rich YSZ green film, we obtained composite films with GDC at 70 μm and YSZ at 7 μm. The obtained films were usually wavy and were flattened by hot pressing with weights. In order to obtain flat films, a two step sintering procedure was adopted and found to be effective. In this process, the first step involved sintering at 1773 K and then the films were re-sintered at 1823 K, pressed under flat alumina plates.

Such a co-fire method may be said to be equivalent to joining separately sintered YSZ and GDC films. However, it is almost impossible to make joining of very thin YSZ (7 μm) and thick GDC (70 μm) films by sintering under pressing: It is only possible by in situ co-fire sintering.

Microstructure and elemental distribution in composite electrolyte. As shown in Fig. 8, the GDC and YSZ layers are densified by our specific method described above. However, arrays of pores always exist at the interface of GDC and YSZ layers. These

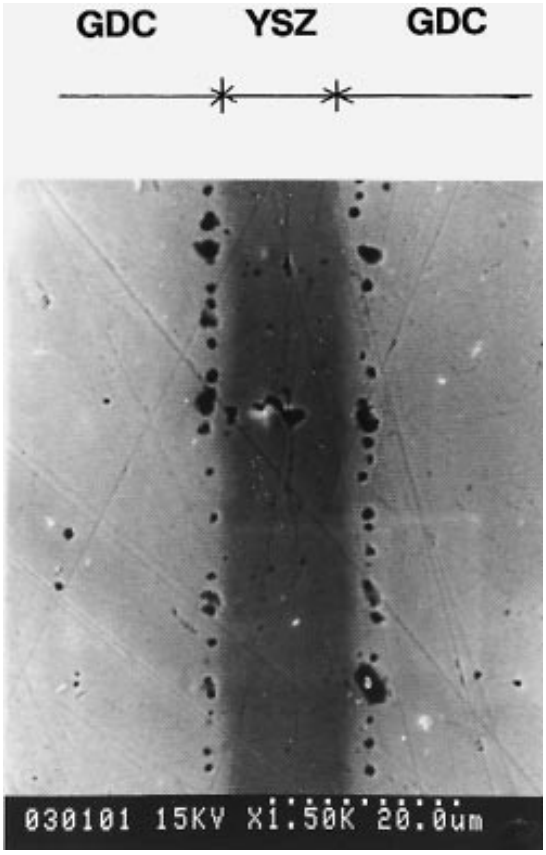

Fig. 8. Scanning Miscroscopy image at the interface of GDC/YSZ/GDC 3 layer composite electrolyte.

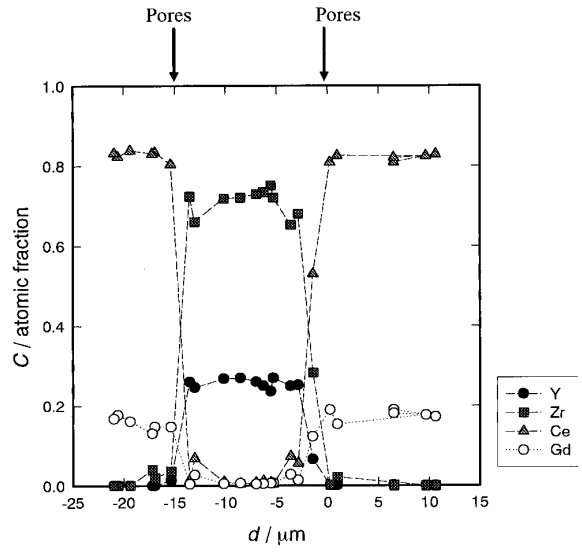

Fig. 9. Elemental distribution of GDC/YSZ/GDC 3 layer composite. ●: distribution of Y, ■: distribution of Zr, ▲: distribution of Ce, ○: distribution of Gd.

pores may be formed in the densification process by the diffusion of Ce and Zr. Figure 9 represents the distribution of elements in the GDC/YSZ/GDC 3 layer composite film (obtained by SEM/EDX), which we believe suggests the formation of a solid solution layer between YSZ and GDC. In Fig. 9, the position of pore arrays are shown in the lines. These lines are in the Ce-rich region, not at the position where $C(\mathrm{Zr})/C(\mathrm{Ce}) = 1$. This phenomenon seems to be due to Kirkendall effect, which is related to the difference of the diffusivity of Ce^{4+}/Gd^{3+} in YSZ and Y^{3+}/Zr^{4+} in GDC. Although a similar phenomenon has been reported by Sakka et al. (1993) [10], more precise analysis will be needed to determine this diffusion process.

4. Conductivity of Composite Electrolyte

4.1. Experimental

Measurements of electrical conductivity. The complex AC impedance spectra in air of co-fired films were measured using an impedance analyzer (SI 1260, Solatron) from 100 mHz to 1M Hz with 10 mV amplitude. The total resistance was obtained from the intercept of the real axis of the arc in the cole-cole plots. On both sides of the electrolyte film, platinum electrodes were pasted with 4 probe platinum wires. The oxygen partial pressure was kept constant, by flowing air at a rate of 100 ml/min. The electrical conductivity was calculated from the resistance, thickness, and electrode area of the films.

4.2. Results

The electrical conductivities of the composite films are summarized as a function of the inverse temperature in Fig. 10. The GDC mono-layer film shows highest conductivity and low activation energy (0.612 eV). The conductivity for the GDC-YSZ-GDC film (GDC/YSZ-4Y 3 layer) is almost the same as for ''YSZ-8Y'', and is better than for ''YSZ-4Y''. The activation energy of the GDC-YSZ-GDC film (0.866 eV) is higher than that of GDC and is slightly lower than that of ''YSZ-8Y'' (0.915 eV). Microstructure of the GDC-YSZ-GDC film (Fig. 8) shows that the thickness of YSZ is about 7 μm and that of GDC was 70 μm. From the thickness of YSZ film, the effect of YSZ on conductivity is estimated to be

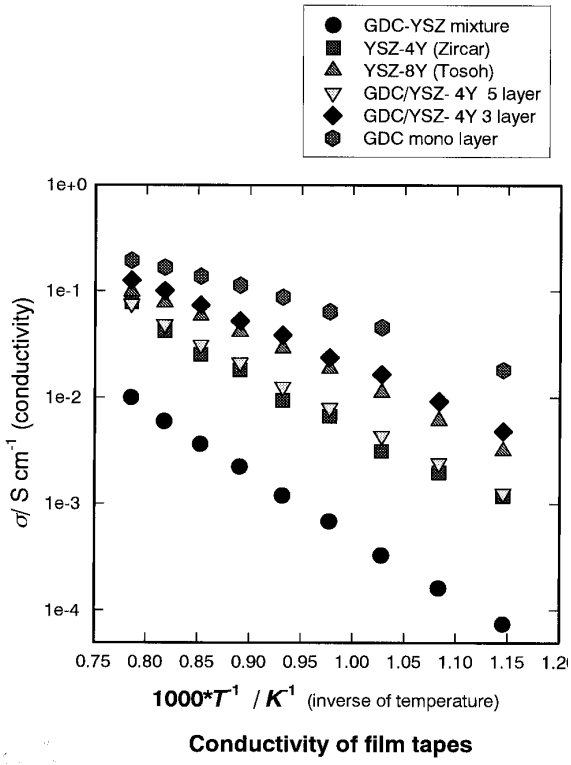

Fig. 10. Conductivity of composite films as a function of the inverse of temperature. ●: GDC-YSZ mixture film, : YSZ-4Y (Zircar), △: YSZ-8Y (Tosoh), ▼: GDC/YSZ-4Y 5 layers composite, ▲: GDC/YSZ-4Y 3 layers composite, ⬮: GDC mono layer.

very little: We can expect almost the same ionic conductivity for GDC-YSZ-GDC composite films as for a GDC mono-layer film. However as shown in Fig. 10, the GDC-YSZ-GDC composite film shows a lower conductivity. The low conductivity comes from the partial exfoliation between GDC and YSZ layer due to TEC mismatch, formation of pores at the GDC-YSZ interface, and formation of GDC-YSZ solid solution.

The insertion of a YSZ-GDC mixed layer (GDC-(YSZ/GDC)-YSZ-(YSZ/GDC)-GDC, 5 layered composite films) was examined to relax mechanical stress due to TEC mismatch. The graded structure would improve the mechanical strength. However, this structure was also not successful, giving poor conductivities and high activation energy (1.06 eV), as shown in Fig. 10. The lower conductivity than GDC-YSZ-GDC 3 layered film comes from many pores both at the YSZ-GDC mixed layer and at the interface between YSZ and GDC layers.

We therefore examined a YSZ/GDC mixture (YSZ:GDC=50:50 mol%) mono-layered film, which also gives unsatisfactory ionic conductivity and high activation energy (1.25 eV) (see Fig. 10). The microstructure of the YSZ-GDC mixture is very porous (estimated to be 20–30% porosity) in the mono-layered films. Hence, the arrays of pores at the interface between GDC and YSZ layers undoubtedly give rise to resistance for ionic conductivity. But it is difficult to conclude that these pores are the main cause of low conductivity, because the volume ratio of pores is not high enough. The GDC-YSZ solid solution may also affect the low conductivity of GDC-YSZ composite films.

5. Discussion

It became clear that the formation of a solid solution is a key factor for the realization of GDC-YSZ-GDC composite electrolyte. In order to prepare the composite films by the co-fire process, the formation of solid solution was inevitable to prevent delamination of component films. It is preferable for composite films to have a structure with graded composition in order to relax the stress raised by the mismatch in TEC. For the graded structure the solid solution phase must be inserted between the single phase films. However, it is likely that the formation of the solid solution reduces the ionic conductivity of GDC-YSZ-GDC composite electrolytes and raises the activation energy for ionic conduction. Ananthapadmanabhan et al. [11] reported that the solid solution in YSZ-YDC system showed lower ionic conductivity and higher activation energy than for YSZ and YDC. Another factor that could reduce the conductivity is the formation of pores at the interface of GDC-YSZ layers in the composite film. Thus the elimination of pores and the formation of very thin solid solution phase should be envisaged for future work.

The lattice expansion of GDC under reducing atmosphere is considered to be a serious problem. According to the estimated oxygen potential profile (Fig. 3), the GDC film on the reducing side will expand, while YSZ and GDC on the oxidizing side do not expand. This expansion is about ten folds than that caused by TEC mismatch. The mismatch due to lattice expansion is reported to be 1–2% between GDC and YSZ [4,12] whereas TEC differences between YSZ

and GDC is about 0.2% at 1273 K. In order to reduce lattice expansion of GDC, the YSZ layer must be faced to the lower oxygen partial pressure side. Thus the YSZ/GDC 2 layer configuration is again proposed, though it is difficult to prepare by co-firing wet process. The alternative candidates may be the following configuration: Anode/YSZ thin layer/GDC thick layer/YSZ thin layer/Cathode. The thin YSZ layer at anode side is expected to reduce the lattice expansion of YSZ-GDC composite film, though the anode/electrolyte overvoltage will increase and TEC mismatch will break the YSZ thin layer as Mehta et al. [15] reported. The co-fire of such a composite film remains for future works and the reproducibility of these composite electrolytes still needs improvement.

6. Conclusion

1. Feasibility of GDC-YSZ-GDC three layer composite film electrolyte was examined by the calculation of oxygen potential profile in the electrolyte. The cell performance of the GDC-YSZ-GDC three layer electrolyte is expected to be better than that of the GDC or the YSZ electrolytes.
2. GDC-YSZ GDC sandwich structured composite films were prepared by a wet co-fire process using binder rich green tape of YSZ and controlling the temperature program.
3. The electrical and/or ionic conductivity of composite films was not as high as the theoretical conductivity due to the presence of a poorly conducting solid solution phase.
4. The formation of the solid solution is a key factor for the production of non-delaminated composite films but degrades the electrical conductivity.
5. Ceria electrolyte is practically difficult to use, due to its poor mechanical strength, TEC mismatch, and lattice expansion in reducing atmospheres.

In the current work, TEC mismatch seems to have been overcome, but the effect of lattice expansion in reducing atmospheres is still a problem for improved mechanical strength, which needs to be achieved in the near future.

References

1. B.C.H. Steele, K. Zheng, R.A. Rudkin, N. Kiratzis and M. Christie, *Proc 4th Intl. Symp. SOFC, Yokohama, 1995*, eds. M. Dokiya, O. Yamamoto, H. Tagawa, and S. Singhal, p. 1028, PV95-1, The Electrochem. Soc. Inc (1995).
2. K. Eguchi, T. Setoguchi, T. Inoue and H. Arai, *Solid State Ionics*, **52**, 165 (1992).
3. M. Gödickemeier, K. Sasaki and L.J. Gauckler, *Proc. 4th Intl. Symp. SOFC, Yokohama, 1995*, eds. M. Dokiya, O. Yamamoto, H. Tagawa and S. Singhal, p. 1072, PV95-1, The Electrochem. Soc. Inc. (1995).
4. M. Mogensen, T. Lindegaard, U.R. Hansen and G. Mogensen, *J. Electrochem. Soc.*, **141**, 2122 (1994).
5. K. Mehta, S.J. Hong, J-F. Jue and A.V. Virkar, *Proc. 3rd Intl. Symp. SOFC, Hawaii, 1993*, eds. S. Singhal and H. Iwahara, p. 92, PV93-4, The Electrochem. Soc. Inc. (1993).
6. S. Choudhury and J.W Patterson, *J. Electrochem. Soc.*, **118**, 1399 (1971).
7. H. Park, R.N. Blumenthal, *J. Electrochem. Soc.*, **136**, 2867, (1989).
8. J. Van herle, T. Horita, T. Kawada, N. Sakai, H. Yokokawa and M. Dokiya, *Proc. 4th Intl. Symp. SOFC, Yokohama, 1995*, eds. M. Dokiya, O. Yamamoto, H. Tagawa and S. Singhal, p. 1082, The Electrochem. Soc. (1995).
9. J. Van herle, T. Horita, T. Kawada, N. Sakai, H. Yokokawa and M. Dokiya, *Solid State Iconics,* **86–88**, pp. 1255–1258 (1996).
10. Y. Sakka, Y. Oishi, K. Ando and Y. Ikeda, *J. Am. Ceram. Soc.*, **76**(5), 1381–1383 (1993).
11. P.V. Ananthapadmanabhan, N. Venkatramani, V.K. Rohatgi, A.C. Momin and K.S. Venkateswarlu, *J. European Ceramic Soc.*, **6**, 111–117 (1990).
12. I. Yasuda and M. Hishinuma, Extended Abstract in Fall Meeting of the Electrochemical Society of Japan, 1F30, p. 139 (1996).